SCIENTIA AGROPECUARIA
Scientia Agropecuaria
Web page: http://revistas.unitru.edu.pe/index.php/scientiaagrop
Facultad de Ciencias Agropecuarias
Universidad Nacional de Trujillo

RESEARCH ARTICLE

Identification of vulnerable areas to flash floods using weighted sum analysis and unsupervised machine learning in arid regions of the northern Atacama Desert

Edwin Pino-Vargas [1]*; German Huayna [2]; Ángel Tapia [2]; Víctor Pocco [1]; Jorge Espinoza-Molina [3]; Fredy Cabrera-Olivera [2]; César Huanacuni-Lupaca [2]; Karina Acosta-Caipa [3]; Lía Ramos-Fernández [4]

[1] Department of Civil Engineering, Jorge Basadre Grohmann National University, Tacna 23000, Peru.
[2] Master's Program in Water Resources, Jorge Basadre Grohmann National University, Tacna 23000, Peru.
[3] Department of Architecture, Jorge Basadre Grohmann National University, Tacna 23000, Peru.
[4] Department of Water Resources, National Agrarian University La Molina, Lima 15024, Peru.

* Corresponding author: epinov@unjbg.edu.pe (E. Pino-Vargas).

Received: 14 November 2024. Accepted: 28 March 2025. Published: 15 April 2025.

Abstract
In recent decades, global warming has triggered significant changes in the hydrological cycle, leading to various disasters, especially contrasting events such as droughts and floods. These occurrences have also been recorded in the Atacama Desert, resulting in considerable economic losses worldwide, in Latin America, in Peru, and within the study region. The primary objective of this study is to obtain fundamental morphometric parameters, including basic spatial, linear, shape, and landscape aspects through the integration of GIS tools and artificial intelligence, enabling the identification of flood-prone areas within micro-watersheds. The studied basin is located at the head of the Atacama Desert, in southern Peru, where various lithological and hydro-geomorphological structures influence its vulnerability to floods. To assess flood vulnerability in the Caplina River micro-watersheds, 16 morphometric parameters were precisely analyzed, identifying areas of high vulnerability that require basin management measures. The results show that the hydrological response of the Caplina Basin is strongly influenced by its morphometric characteristics, with micro-watersheds in the middle and lower sections exhibiting higher susceptibility to flash floods. These findings aim to support urban planning and watershed management, offering insights for policymakers to develop flood mitigation strategies and enhance infrastructure resilience.

Keywords: Flash floods; Caplina Basin; Weighted Sum Analysis; Unsupervised Machine Learning; Atacama Desert.

DOI: https://doi.org/10.17268/sci.agropecu.2025.020

Cite this article:
Pino-Vargas, E., Huayna, G., Tapia, A., Pocco, V., Espinoza-Molina, J., Cabrera-Olivera, F., Huanacuni-Lupaca, C., Acosta-Caipa, K., & Ramos-Fernández, L. (2025). Identification of vulnerable areas to flash floods using weighted sum analysis and unsupervised machine learning in arid regions of the northern Atacama Desert. *Scientia Agropecuaria*, *16*(2), 249-261.

1. Introduction

The increase in Earth's surface temperature globally over recent decades has created an energy imbalance on our planet, leading to alterations in the hydrological cycle that cause droughts, floods, wildfires, and climate change (Adeyeri et al., 2024). Climate change projections indicate negative impacts on hydrological systems, with significant changes in precipitation and temperature worldwide (Pino-Vargas & Chávarri-Velarde, 2022; Wei et al., 2021). Globally, floods pose natural hazards with adverse environmental and socioeconomic impacts (Kalogeropoulos et al., 2023).

Over recent decades, extreme flood events and their intensities have increased in most regions, mainly driven by climate change (Fernández-Nóvoa et al., 2024). Natural disasters, including earthquakes, floods, cyclones, hurricanes, droughts, and wildfires, cause yearly damages of about $300 billion globally, with an annual growth trend of 5% to 7% (Rentschler et al., 2022). Notably, 23% of the world's population is exposed to flood risks (Rentschler et al., 2022). The detrimental effects of floods on agriculture are evident in the destruction or impairment of crops.

Latin America and the Caribbean (LAC), like many other world regions, are prone to hydro-meteorological disasters that threaten livelihoods and cause economic losses (Pinos & Quesada-Román, 2021). In South America, increased extreme rainfall has been associated with more frequent floods, although recent studies suggest that reduced soil moisture might have the opposite effect (Brêda et al., 2023). Multiple factors drive flood hazards and risks, and there is considerable uncertainty in assessments, particularly in future projections (Kundzewicz et al., 2019). Floods are the most widespread, environmentally diverse, and continually destructive natural hazard (Roldán et al., 2022).

In Peru, due to its geomorphological and geological situation, it is highly exposed to various risks, including floods caused by the El Niño phenomenon and earthquakes that severely affect the population (Porto de Albuquerque et al., 2023). Floods occur due to excessive rainfall, as well as infrastructure collapse, seasonal snowmelt, and volcanic eruption-induced flooding. Other social factors, such as changes in land cover from human activities, waste dumping, inadequate land management, deforestation, urbanization, and improper river channeling, also contribute to these phenomena (Porto de Albuquerque et al., 2023).

The Atacama Desert located in northern Chile and southern Peru, is the oldest and driest non-polar temperate desert on Earth (Bull et al., 2018). In recent years, extraordinary precipitation events have been recorded across various regions of the Atacama Desert, forming small surface lakes in areas where it was previously believed that no rain fell (Roldán et al., 2022). In the northern region of the desert, extraordinary precipitation events have led to surface storage, vegetation growth, and debris flows in previously dry areas (Pino-Vargas & Chávarri-Velarde, 2022). In hyper-arid regions, meteorological threats can develop rapidly, leading to catastrophes (Roldán et al., 2022).

The most used method to assess flood risks relies on predicting the magnitude and extent of 100- or 200-year floods. However, this approach can be misleading, as areas outside these boundaries are assumed to be free from risk. In this context, a geomorphological approach is especially useful (Thompson & Clayton, 2002). The flood risk distribution in riverine areas is not uniform, so correlations are established among various geomorphological variables to evaluate land vulnerability. River channel and terrain geomorphology play an essential role in river overflow and flooding (Aggarwal et al., 2024). When based on geomorphology, Early Warning Systems (EWS) are widely recognized as one of the best tools for risk prevention, mitigation, preparation, and response strategies (Piacentini et al., 2020).

In many parts of the world, sediment transport and morphological changes in freshwater environments, such as rivers, are only marginally considered. This can lead to potentially erroneous estimates of flood impacts. Sediment significantly increases flood risk (Liu et al., 2022). It is essential to pay attention to sediment transport since these play a vital role in the morphological response of river channels during major floods (Vázquez-Tarrío et al., 2024).

In this way, various studies have analyzed the susceptibility of areas to flooding using Multi-Criteria Decision Analysis (MCDA) approaches (Abdelkareem & Mansour, 2023; Riaz & Mohiuddin, 2025). This study aims to identify flash flood-vulnerable areas in the Caplina Basin employing Geographic Information Systems (GIS) supported by Weighted Sum Analysis (WSA) and unsupervised Principal Component Analysis (PCA) as processing tools, to assess which method provides a more accurate and effective prioritization of vulnerable areas.

2. Methodology

2.1 Study Area

The study area was in the Tacna region, at the head of the Atacama Desert. The region is characterized by an arid climate, with minimal annual precipitation, characteristic of the driest deserts in the world (Machaca-Pillaca et al., 2022). The Caplina River basin is part of the Peruvian Pacific hydrological unit and extends between the geographical coordinates of 18°35′ to 17°56′ south latitude and 70°67′ to 69°75′ west longitude (Figure 1). Within this basin, three sub-basins have been identified: Caplina, Uchusuma, and Los Molles, collectively covering an area of 2,224 km². The headwaters of the basin reach a maximum elevation of 5,685 meters above sea level in the western cordillera, and the rivers within these sub-basins exhibit an endorheic drainage pattern (Ovalle & Begazo, 2016). The study obtained fundamental morphometric parameters, including basic spatial aspects, linear aspects, shape aspects, and landscape aspects, using the QGIS environment. Derived or secondary parameters, which influence the drainage network, basin geometry, drainage texture, and relief of the selected basins, are detailed in Table 1, respectively, where fifteen micro-watersheds were delineated. The prioritization of micro-watersheds employed two approaches: principal component analysis (PCA), using Jupyter Notebooks and Python programming language, and weighted. The prioritization of micro-watersheds for assessing their vulnerability to flash flood events was conducted by comparing both approaches employed (Figure 2).

2.2 Data Source

The digital elevation model (DEM) from the Shuttle Radar Topography Mission (SRTM) with a 1-arc-second resolution (approximately 30 meters spatial resolution) was used (Farr et al., 2007). The digital elevation models were obtained through Google Earth Engine (GEE), a cloud-based platform providing access to an extensive catalog of public geospatial data, including satellite and aerial imagery and environmental, meteorological, climate, topographic, and land cover variables (Amani et al., 2020; Safanelli et al., 2020).

2.3 Morphometric Parameters

For the morphometric characterization of the basin geometry, the following measurements were taken: (i) linear aspect, (ii) shape aspect, and (iii) landscape aspect. The linear aspect includes drainage density (Dd), stream frequency (Fs), texture ratio (Tr), and flow length (Lg). The shape parameter incorporates elongation ratio (Er), form factor (Ff), circularity ratio (Cr), compactness coefficient (Cc), and shape index (Sf). The landscape parameter includes relative relief (Rh), relief and sub-basin slope (As), basin relief (R), and unit hypsometric curve (Hi) (Table 1).

2.4 Weighted Sum Analysis (WSA)

The WSA approach is widely accepted for tackling complex issues, offering a consistent method to compare surface processes of related entities, like drainage basins, making it effective for classifying and prioritizing critical sub-basins in water-scarce areas (Kadam et al., 2019; Kumar et al., 2022). Many researchers widely employ this method to support sustainable planning and management of sub-basins, especially in areas with limited data (Altaf et al., 2014).

WSA reflects decision-makers' preferences through an additive linear function, with the best option being the one with the highest score after transforming all evaluation criteria into a single dimension. This is represented in the following equation 1.

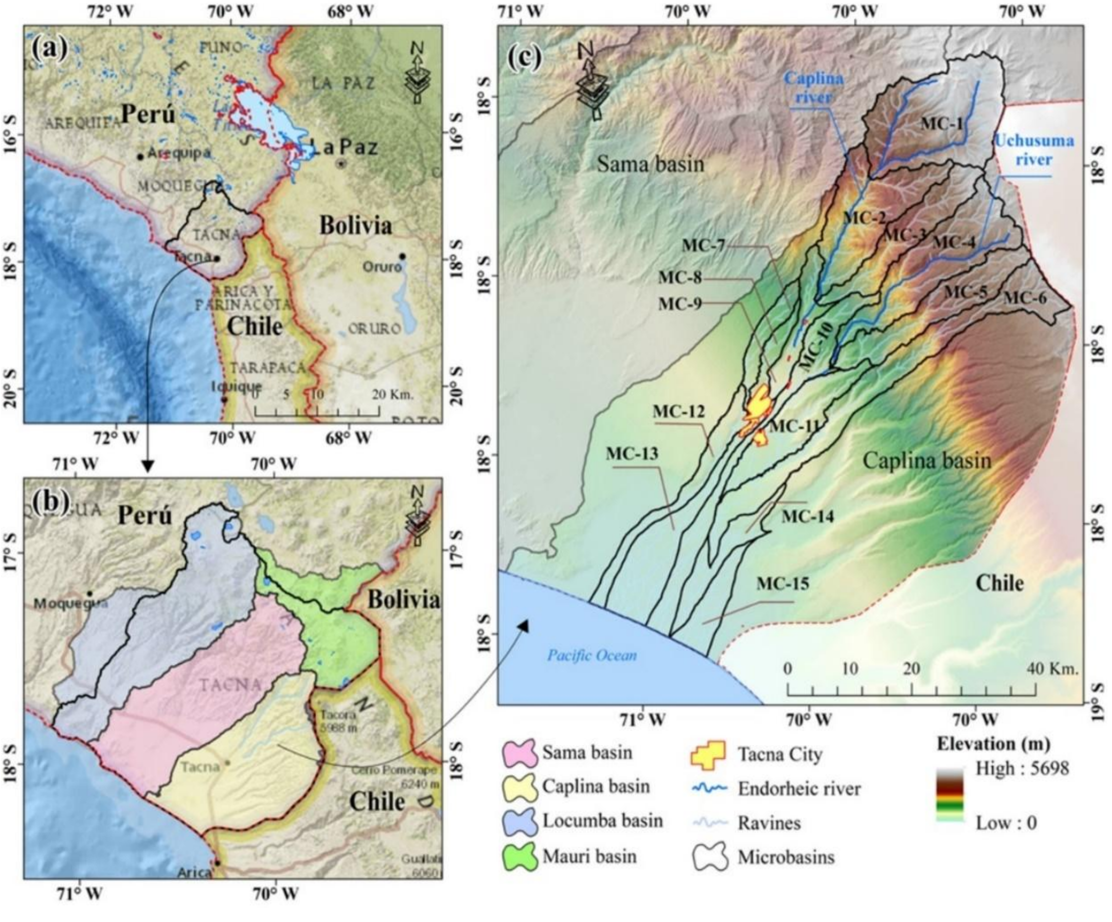

Figure 1. Location map of the study area. (a) Location in South America. (b) Adjacent basin system in the region, including the Sama, Mauri, Caplina, and Locumba basins. (c) Location of micro-watersheds MC: 1 to 15 within the Caplina basin.

Table 1
Formulas adopted to determine the morphometric parameters and associated references

Morphometric parameters	Formula and Definition	References
Areal aspect		
Area (A)	Area of watershed in (km^2), GIS analysis	
Perimeter (P)	Perimeter of watershed in (km), GIS analysis	
Basin length (L_b)	$L_b = 1.312 * A^{0.568}$, A = area of the basin (km^2)	(Sreedevi et al., 2013)
Stream order (U)	Hierarchical rank, GIS analysis	(Strahler, 1964)
Stream length (L_u)	Length of the stream (km) of order u	(Horton, 1945)
Linear aspect		
Drainage density (D_d)	$D_d = L_U/A$ Where L_u= total stream length of all orders, A = area of the basin (km^2)	(Horton, 1932)
Stream frequency (F_s)	$F_S = N_U/A$, Where N_u= total no. of streams of all orders, A = area of the basin (km^2)	(Horton, 1932)
Length of overland flow (L_g)	$L_g = 1/(D_d * 2)$ Where D_d= Drainage density	(Horton, 1945)
Ratio texture (T_r)	$T_r = N_i/P$ Where N_i= total no. of first order streams, P = perimeter of the basin	(Horton, 1945)
Shape aspect		
Elongation ratio (E_r)	$E_r = 2\sqrt{(A/\pi)}\,/L_b$ Where A = area of the basin (km^2), L_b = basin length, π = 3.14	(Schumm, 1956)
From factor (F_f)	$F_f = A/{L_b}^2$ Where A = area of the basin (km^2), ${L_b}^2$ = square of basin length	(Horton, 1945)
Circularity ratio (C_r)	$C_r = 4\pi * A/P^2$ Where A = area of the basin (km^2), P^2 = square of perimeter (km)	(Miller, 1953)
Compactness coefficient (C_c)	$C_C = 0.2841 * (P/A)^2$ Where P = perimeter of basin (km), A = area of the basin (km2)	(Gravelius et al., 1914)
Shape factor (S_f)	$S_f = {L_b}^2/A$ Where ${L_b}^2$ = square of basin length, A = area of the basin (km^2),	(Horton, 1932)
Relief aspect		
Relief ratio (R_h)	$R_h = H/L_b$ Where H=total relief (relative relief) of the basin in km, L_b=basin length	(Schumm, 1956)
Basin relief (R)	Diference between maximum and minimum elevation of watershed	(Schumm, 1956)
Average slope (A_s)	In degree, GIS analysis	
Hypsometric integral	$H_i = (E_{mean} - E_{min})/(E_{max} - E_{min})$	(Pike & Wilson, 1971)

$$WSA = Pr_{p1} * W_{p1} + Pr_{p2} * W_{p2} + \ ... + Pr_n * W_n \quad (1)$$

Where WSA is the composite parameter for weighted sum analysis, Pr is the preliminary priority rank of each morphometric parameter (p1, p2, ..., n), and W indicates the weight of the morphometric parameters obtained by cross-correlation analysis, expressed as follows:

$$\mathrm{W} = \frac{Sum\ of\ correlation\ coefficient}{Grand\ total\ of\ correlations} \quad (2)$$

2.5 Principal Component Analysis (PCA)

PCA is a popular dimensionality reduction technique used in statistics and machine learning to improve feature accuracy while reducing processing time and retaining essential information (Velliangiri et al., 2019). PCA has been widely used for handling high-dimensional datasets to condense information, maintaining most of its variability (Kumar et al., 2022; Sharma et al., 2023). PCA selects the most significant features by transforming the original variables into a set of uncorrelated variables, called principal components (PCs) (Wold et al., 1987).

These components explain most of the variance in the parameters, with the first principal component (PC1) contributing most to the total variance, followed by the second (PC2), which maximizes its contribution to the residual difference and is uncorrelated with the first. Subsequent components are calculated similarly. This method's primary criterion relies on a complete change of the initial parameters, with principal components obtained using a loading factor and rotation matrices.

3. Results and discussion

Morphometric basin analysis can effectively prioritize areas with high flash flood risk, assisting in watershed management planning. This study employed various morphometric parameters affecting a basin's hydrological response to prioritize the Caplina River micro-watersheds based on flash flood vulnerability.

3.1 Morphometric parameters

Morphometric analysis was conducted for 15 micro-watersheds, considering the drainage network of the entire study area as a fifth-order basin (Figure 3a). This analysis included 18 parameters for each micro-watershed to determine their dimensions, shape, area, and drainage network characteristics. The results show that Micro-watershed 8 is the smallest, with an area of 39.43 km², while Micro-watershed 1 is the largest, with an area of 325.49 km² (Table 2).

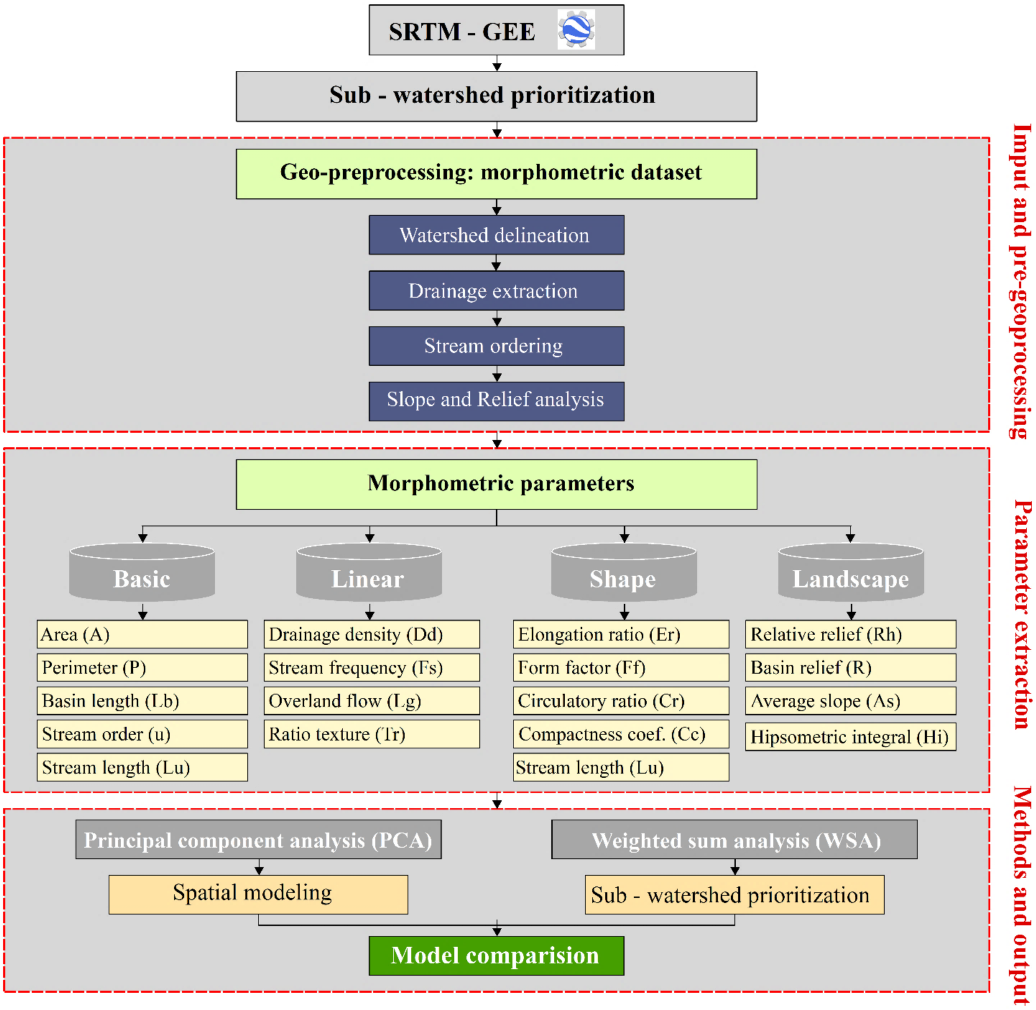

Figure 2. Flowchart of the methodology for processing micro-watershed prioritization.

Over a third of the sub-watersheds have areas larger than 150 km². The small size of micro-watersheds in the study area directly influences their vulnerability to flash floods (Balica et al., 2009).
Additionally, 722 channels were identified, with a total length of 1703.34 km. Dimensional measures, such as area, perimeter, basin length, average slope, and elevations, are detailed in Table 2. Basic drainage characteristics, including stream order, stream count, and stream length, are shown in Table S1 (see Supplementary Material).

3.1.1 Linear parameters

Drainage density (Dd) is defined as the total length of stream segments per unit area. It primarily depends on surface topography, drainage system, distance, fluid viscosity, gravitational acceleration, and scale factor. Weathering resistance, permeability, rock composition, landscape, and vegetation also influence drainage density (Zheng et al., 2021). Low Dd values are observed in permeable areas with dense vegetation and gentle topography, while high Dd values occur in weak and impermeable soils with sparse vegetation and mountainous terrain. Micro-watersheds 1, 2, 3, and 4 have low Dd values, ranging from 0.516 to 0.610 per km², categorized as very coarse Dd, while Micro-watersheds 13, 14, and 15 show high Dd, ranging from 1.007 to 1.162 km². Figure 3b illustrates Dd's spatial distribution, indicating a high density in the southern part of the sub-basin.
Stream frequency (Fs) is inversely related to permeability and directly related to basin roughness. Fs primarily depends on surface lithological and physiographic conditions, along with precipitation in the specific area (Hynek et al., 2022). High stream frequency suggests superficial rock presence, complex lithological conditions, and low permeability, leading to higher erosion, while low frequency indicates higher permeability and

lower erosion. The Fs of the micro-watersheds varies from 0.21 to 0.53 per km², as shown in (Figure 3c). Low Fs values are found in Hydrographic Basins 3, 4, 5, 6, and 11, resulting in reduced surface runoff, while high Fs values are observed in Basins 1, 2, 7, 8, 9, 10, 12, 13, 14, and 15 (Table 3). High Fs in these basins implies low water infiltration, thus increasing surface runoff and vegetation presence.

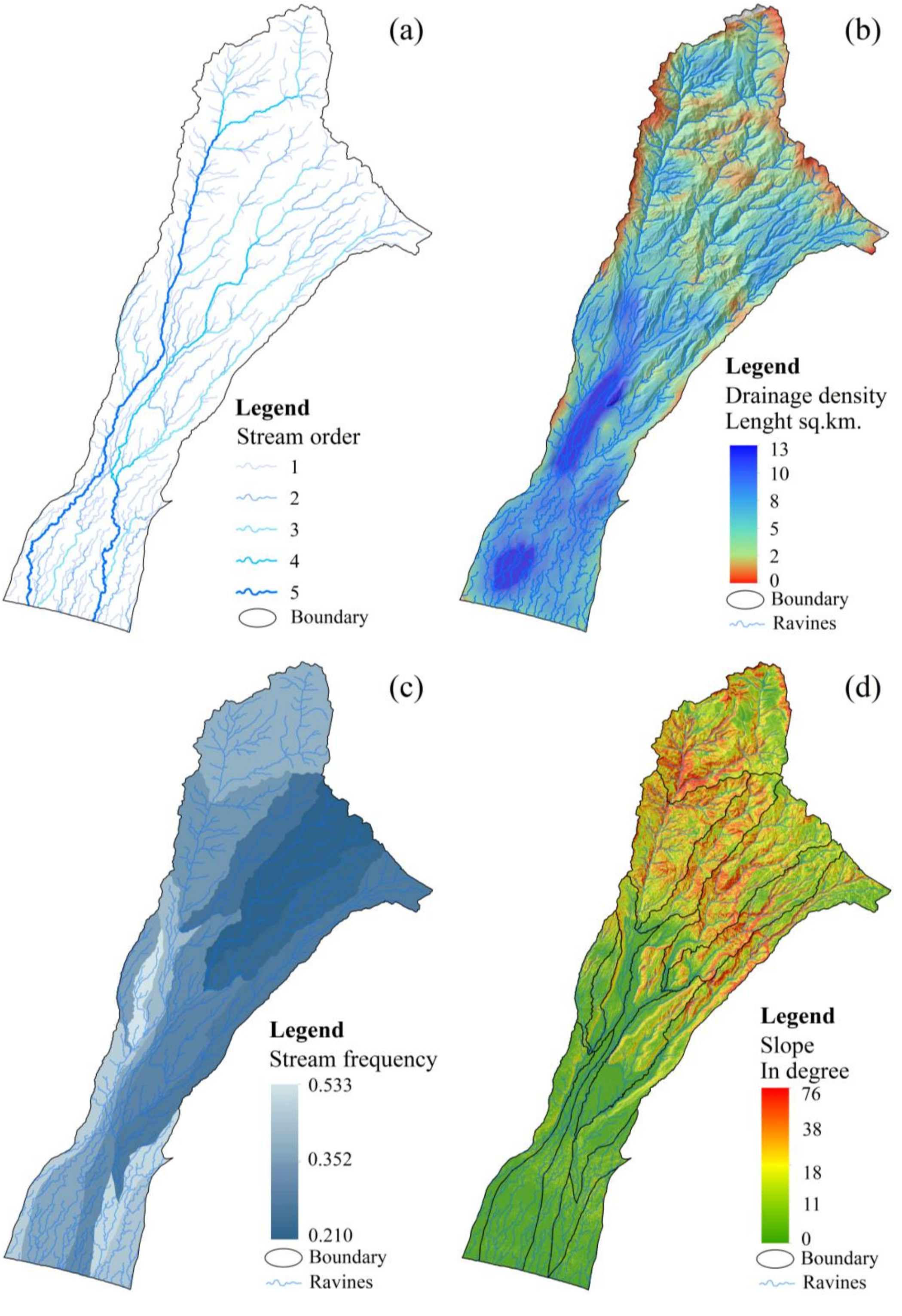

Figure 3. Map of the studied basin: (a) Drainage order; (b) drainage density; (c) stream frequency; and (d) slope.

Table 2
Detailed description of the territorial, linear and landscape characteristics of the micro-basins of the Caplina

Name	Area (km2)	Perimeter (km)	Total No. Streams	Basin Length (km)	Average Slope (degrees)	Elevation (m)		
						Max	Min	Mean
MC-1	315.49	84.71	116	34.46	21.94	5685	2290	4205
MC-2	215.78	92.21	66	27.77	22.93	4584	1236	2592
MC-3	137.17	83.49	38	21.47	22.49	4814	1236	3060
MC-4	238.41	108.74	50	29.39	20.77	4958	982	3209
MC-5	158.98	93.72	42	23.35	18.91	4506	981	2837
MC-6	273.81	179.39	78	31.80	14.88	4537	110	1980
MC-7	51.16	55.86	18	12.26	10.75	1941	530	1196
MC-8	39.43	47.98	21	10.58	8.79	1607	531	1027
MC-9	74.39	74.94	31	15.17	9.83	2122	546	1170
MC-10	174.78	152.66	53	24.64	8.12	2251	4	663
MC-11	140.54	81.41	41	21.77	10.06	1724	250	703
MC-12	93.12	97.50	41	17.23	6.10	928	0	350
MC-13	161.13	96.46	59	23.53	3.88	694	0	140
MC-14	79.55	77.03	37	15.76	6.13	667	8	196
MC-15	71.21	49.59	31	14.80	6.08	268	0	80

Table 3
Morphometric parameters directly and inversely proportional to the flash flood risk

Microbasin Code	Directly Proportional							Inversely Proportional				
	Dd	Fs	Cr	Tr	As	R	Rh	Er	Ff	Sf	Cc	Lg
MC-1	0.588	0.368	0.553	0.366	21.941	3.395	0.099	0.582	0.266	3.765	1.345	0.850
MC-2	0.610	0.306	0.319	0.380	22.928	3.348	0.121	0.597	0.280	3.575	1.771	0.820
MC-3	0.516	0.277	0.247	0.240	22.486	3.578	0.167	0.616	0.297	3.361	2.011	0.969
MC-4	0.578	0.210	0.253	0.276	20.773	3.976	0.135	0.593	0.276	3.624	1.987	0.866
MC-5	0.722	0.264	0.227	0.235	18.912	3.525	0.151	0.609	0.292	3.430	2.097	0.692
MC-6	0.722	0.285	0.107	0.240	14.884	4.427	0.139	0.587	0.271	3.693	3.058	0.693
MC-7	0.938	0.352	0.206	0.179	10.753	1.411	0.115	0.658	0.340	2.940	2.203	0.533
MC-8	0.972	0.533	0.215	0.250	8.793	1.076	0.102	0.670	0.352	2.837	2.156	0.514
MC-9	0.900	0.417	0.166	0.254	9.833	1.576	0.104	0.642	0.323	3.093	2.451	0.555
MC-10	1.020	0.303	0.094	0.242	8.120	2.247	0.091	0.606	0.288	3.474	3.258	0.490
MC-11	0.829	0.292	0.267	0.270	10.056	1.474	0.068	0.615	0.297	3.373	1.937	0.603
MC-12	0.799	0.440	0.123	0.287	6.099	0.928	0.054	0.632	0.314	3.189	2.850	0.626
MC-13	1.162	0.366	0.218	0.425	3.884	0.694	0.029	0.609	0.291	3.436	2.144	0.430
MC-14	1.055	0.465	0.168	0.338	6.134	0.659	0.042	0.639	0.320	3.121	2.436	0.474
MC-15	1.007	0.435	0.364	0.423	6.078	0.268	0.018	0.644	0.325	3.075	1.658	0.496

Note: Dd—drainage density; Fs—stream frequency; Cr—circulatory ratio; Tr—ratio texture; As—average slope in degrees; R—basin relief; Rh—relative relief in meters; Er—elongation ratio; Ff—form factor; Sf—shape factor; Cc—compactness coefficient; Lg—length of overland flow.

Flow length (Lg) is the distance water travels across the land surface before concentrating in specific channels, influencing the basin's hydrological and geographical development (Horton, 1945). Lg values range from 0.43 to 0.96 (Table 3). Micro-watersheds 1 to 6, characterized by relatively high Lg values, have extended flow paths with reduced runoff, while Micro-watersheds 7 to 15, with lower Lg values, imply quick surface runoff entry into channels, making them highly vulnerable to floods due to reduced water percolation (Bush et al., 2020).

Texture ratio (Tr) is the ratio of total stream segments to the basin's perimeter (Horton, 1945), indicating the relative spacing of channels per unit basin area. The perimeter is highly significant in basin geomorphology. Texture ratio depends on the basin's geomorphic development, underlying lithology, soil type, vegetation pattern, precipitation quantity, and basin relief (Smith, 1950). Generally, low Tr values indicate moderate to low texture, whereas high Tr values indicate high texture.

3.1.2 Shape parameters

Elongation ratio (Er) generally ranges from 0.6 to 1 across different geological and climatic contexts (Strahler, 1964). In areas with steep slopes and high relief, Er varies between 0.6 and 0.8. The elongation ratio of the studied micro-watersheds ranges from 0.58 to 0.67, indicating lower basin elongation, high gradient and elevation, and moderate structural influence (Sreelakshmy et al., 2023).

Form factor (Ff) is the ratio between basin area and the square of its length, suggests that an elongated basin has a proportional form factor (Strahler, 1964). A basin with an Ff of 1 is circular, while one with an Ff of 0 is elongated. The studied micro-watersheds' Ff values range from 0.26 to 0.35, indicating all micro-watersheds are elongated.

Circularity ratio (Cr) is the ratio between the basin area and the area of a circle with the same perimeter, which ranges from 0 to 1. Cr values per micro-watershed are detailed in Table 3.

Compactness coefficient (Cc) is defined as the ratio between the basin perimeter and the circumference of a circle with the same area as the basin, represented in square kilometers (Horton, 1945). The highest compactness coefficient is observed in Micro-watershed 10, and the lowest in Micro-watershed 1 (Table 3).

Shape index (Sf) represents the inverse of stream frequency, reflects stream spacing within the river basin. A high value suggests wide stream distribution spacing (Yadav et al., 2020). The form factor for the micro-watershed is between 2.9 and 3.7, indicating relatively high stream spacing.

3.1.3 Landscape parameters

Relative relief (Rh) is calculated by dividing the total basin relief by its length. This value helps assess the basin slope and estimate runoff generation and erosion intensity within the basin. Basin size and drainage area are inversely related to relief ratio, with Rh values of the micro-watersheds shown in Table 3. Basin relief (R) refers to the elevation difference between the highest and lowest points within the basin. R has a significant impact on flood characteristics and sediment or material transport potential. It is one of the key factors influencing stream gradient and can be used to analyze the basin's denudation characteristics (Sreedevi et al., 2013). Low R values indicate conditions conducive to runoff generation and debris movement within basins (Table 3). Slope (As) of the terrain is correlated with soil erosion capacity and negatively correlated with infiltration capacity (Mahala, 2020). Higher slope percentages result in increased erosion within a basin, assuming other variables remain constant. Lower slopes promote higher infiltration compared to steeper slopes. The steepest slopes are found in the upper-middle basin areas (Figure 3d).

3.2 Hypsometric Curve

The hypsometric curve allows for comparison of prior erosive environments among different basins that share similar climatic conditions and have approximately equivalent areas (Willgoose, 1994). Young landforms (in an unbalanced phase) exhibit convex-upward curves with a Hi greater than 0.6, while mature landforms (in equilibrium) show S-shaped curves with a Hi between 0.3 and 0.6. Severely eroded ancient landforms have concave-upward curves with a Hi below 0.3. Micro-watershed 13 is in an ancient and eroded stage, micro-watersheds 1, 3, 4, 5, 7, and 8 are young, and micro-watersheds 2, 6, 9, 10, 11, 12, 14, and 15 have a mature relief (Figure 4).

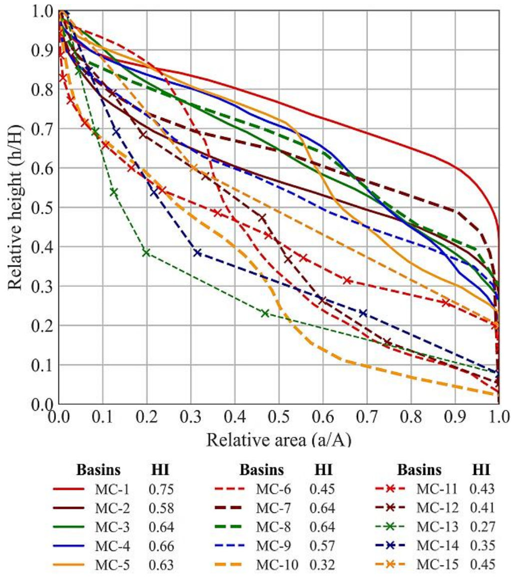

Figure 4. Family of hypsometric curves showing ideal stages of fluvial development in the Caplina River sub-watersheds.

3.3 Assignment of preliminary priority classifications for sub-basins

The morphometric parameters Dd, Fs, Cr, Tr, As, R, and Rh (Table 3) are directly related to flash flood vulnerability. Similarly, Er, Ff, Sf, Cc, and Lg (Table 3) show an inverse relationship with flash flood vulnerability. After this analysis, priorities were assigned from highest to lowest, with Rank 1 for the micro-watershed having the highest parameter value and Rank 15 for the micro-watershed with the lowest parameter value, as shown in Table S2 (see Supplementary Material). Using the obtained parameters, a correlation matrix of the 12 variables was generated to determine the interrelationships between the various morphometric parameters, see Table S3 (see Supplementary Material). The preliminary priority rankings were used for this estimation. The statistical correlation matrix shows that Dd has a positive correlation with Fs, Tr, Sf, and Lg, meaning higher values indicate greater flood vulnerability, and vice versa with Cr, As, R, Rh, Er, Ft, and Cc, where higher values correspond to lower flash flood vulnerability.

3.4 Final Ranking Using Weighted Sum Analysis (WSA)

The morphometric parameter values, calculated using Equation 1, were determined by their importance using the weighted sum model. This process utilized the preliminary priority values and the final weights of each morphometric parameter.

For example, the WSAcp value of Dd (MC1) was obtained by multiplying 13 × 0.12 = 1.56, similarly for all subsequent WSAcp values. Each parameter has a corresponding weight (w). The WSAcp values are shown in Table S4 (see Supplementary Material).

Additionally, a model based on the composite weighted sum (WSAcp) values of various morphometric parameters was developed to determine the final sub-basin priority rankings for flash flood vulnerability. The parameters were grouped into two categories: those with a direct and those with an indirect influence on flooding. Priority was calculated by subtracting the composite values of both groups, with the micro-watersheds with the lowest values receiving the highest priority rankings. The WSA model (Table 4) indicates that Micro-watersheds 1, 6, and 10 have higher priorities with lower preliminary rankings, while Micro-watersheds 7, 8, and 15 with lower priority values have higher rankings, respectively. The results suggest that the middle part of the sub-basin is highly vulnerable to flash floods.

3.5 Final ranking using Principal Component Analysis (PCA)

PCA identifies priority flood parameters, demonstrating the correlation between criteria. This study produces a PCA load matrix showing the intensity of the relationship or association between the factors, parameters, and associated variables (Jolliffe & Cadima, 2016). PCA analyzed the most significant components, reducing the 12 parameters to three principal components (PCs). PCA then generates, through orthogonal transformations, the load matrix of the first element and the rotated load matrix, extracting 12 morphometric parameters from the initial unrotated factor load matrix. Table S5 (see Supplementary Material) shows that around 93.1% of the total variance of the variables comprises the first three components. In Table S6 (see Supplementary Material), the first variable in PC1 is highly correlated (>0.90) with As and R, moderately correlated (>0.75) with Dd, Fs, As, Rh, Er, Ff, Sf, and Lg. PC2 is highly correlated with Cr, Tr, and partially associated with Cc, while PC3 has a low correlation (<0.53) with all other variables of the Caplina River Basin.

Some factors are strongly correlated with other variables, while some show moderate or low correlations with others. However, it is challenging to define a substantially significant component at this point. Therefore, the load matrix of the first element is rotated for better interpretation to overcome the difficulty of identifying a significant variable signal. After multiplying the transformation matrix by the load matrix of the selected first factor component, the rotated factor load matrix is generated. The first component (>0.90) is highly correlated with Rh and moderately associated with Dd, Lg, and R, as shown in Table S6 (see Supplementary Material).

The second component is strongly correlated with Ef and Sf and Sr, with a low correlation with all remaining variables. The third component has a high correlation (>0.90) with Cc and Cr, with insignificant correlations for the remaining variables. This third component can be considered an organizational process factor for the Caplina River Basin. As shown in Table S6 (see Supplementary Material), three relevant parameters—Rh, Ff, and Cc—were finally used for sub-basin prioritization because they are not interrelated (Figure 5).

In this context, principal component analysis applies to all morphometric variables to derive principal components and determine the most effective prioritization (Meshram & Sharma, 2017).

Table 4
Final ranking and micro-basin priority areas

Microbasin Code	WSAcp (+)	WSAcp (-)	Priory	Final Priority Ranks	Priory Type
MC-1	0.29	-3.89	4.18	13	Very low
MC-2	0.33	-1.34	1.67	7	Medium
MC-3	2.63	2.22	0.41	5	High
MC-4	1.41	-1.57	2.98	11	Low
MC-5	4.33	1.94	2.39	10	Low
MC-6	6.02	0.98	5.04	15	Very low
MC-7	7.17	7.57	-0.39	3	Very high
MC-8	6.96	7.98	-1.02	1	Very high
MC-9	6.79	6.86	-0.07	4	High
MC-10	8.68	4.07	4.60	14	Low
MC-11	3.63	1.86	1.77	9	Medium
MC-12	7.44	5.72	1.72	8	Medium
MC-13	6.09	2.75	3.34	12	Low
MC-14	7.53	6.56	0.96	6	High
MC-15	4.23	4.74	-0.51	2	Very high

Table 5 reveals that Micro-watersheds 12 and 14 maintain a low general Cp rating of 4.33 ranking (1,2) with very high priority, while Micro-watershed 1 receives a maximum Cp of 12.33 ranking (15) and, therefore, the lowest priority. The difference between flood vulnerability and potential interventions is of utmost importance. The priority map of the Caplina River micro-watershed in Figure 6 indicates that protection measures for debris flows in Micro-watersheds 7 and 8 could extend to 9, 10, and other sub-watersheds according to the priority classification.

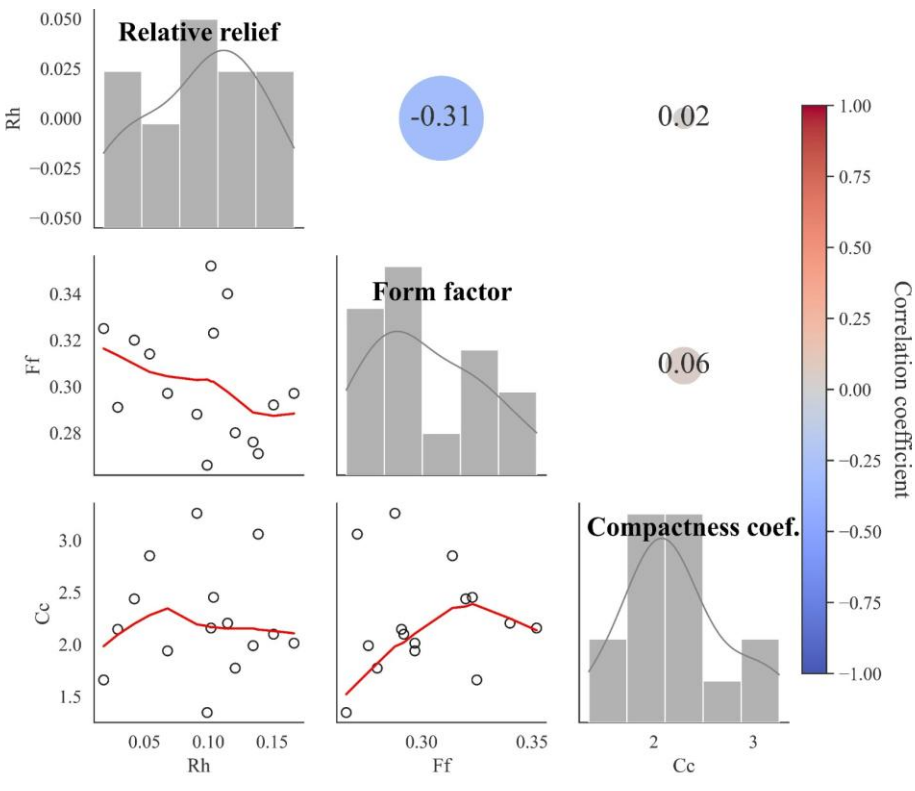

Figure 5. Inter-correlation between morphometric parameters used for prioritization based on the PCA method.

Table 5
Results and final prioritization ranking of sub-watersheds using PCA

Watershed code	Rh	Ff	Cc	Compound parameter	Final Priority Ranks	Priory Type
MC-1	7	15	15	12.33	15	Very low
MC-2	11	12	13	12.00	13	Very low
MC-3	15	7	10	10.67	11	Low
MC-4	12	13	11	12.00	14	Very low
MC-5	14	9	9	10.67	12	Low
MC-6	13	14	2	9.67	10	Low
MC-7	10	2	6	6	5	High
MC-8	8	1	7	5.33	3	Very high
MC-9	9	4	4	5.67	4	High
MC-10	6	11	1	6.00	6	High
MC-11	5	8	12	8.33	9	Medium
MC-12	4	6	3	4.33	1	Very high
MC-13	2	10	8	6.67	8	Medium
MC-14	3	5	5	4.33	2	Very high
MC-15	1	3	14	6	7	Medium

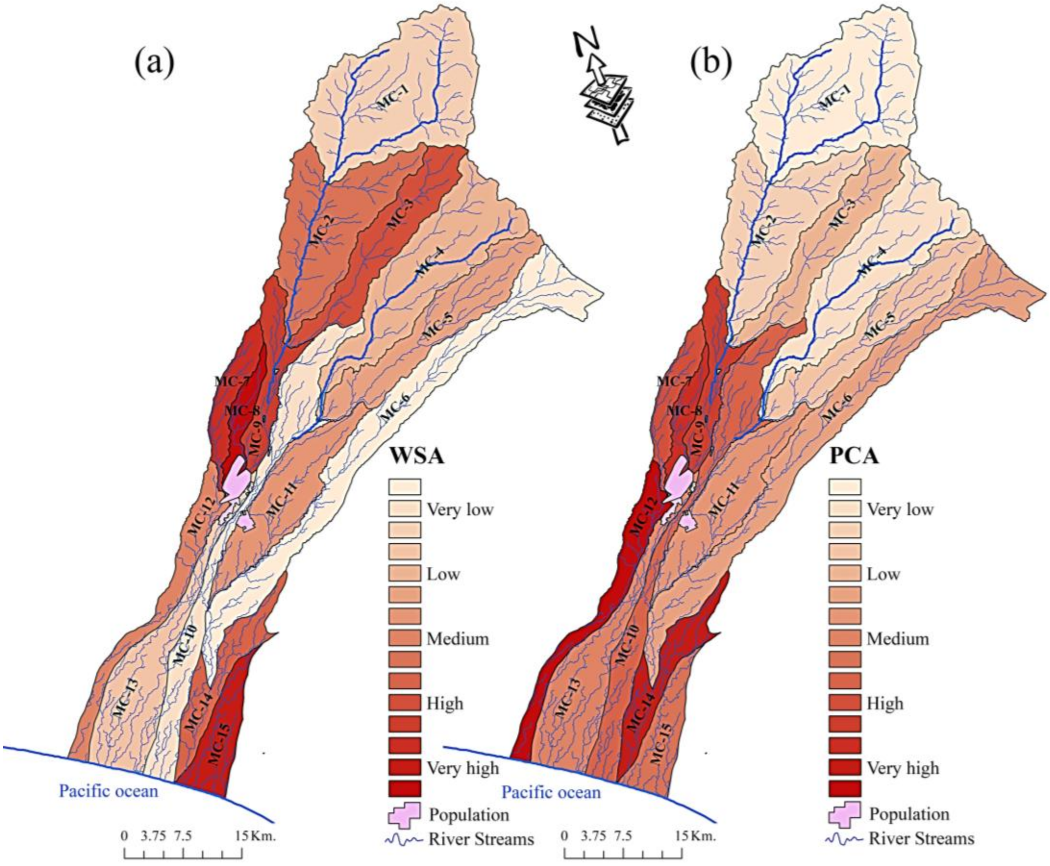

Figure 6. Prioritization of micro-watersheds map (a) WSA method; and (b) PCA method.

4. Conclusions

This study prioritized fifteen micro-watersheds and identified areas vulnerable to flash floods during extreme events based on linear, aerial, and landscape morphometric parameters derived from a digital elevation model (DEM). The efficiency of advanced quantitative and geospatial techniques using a GIS was demonstrated, enhancing the study's reliability in micro-watersheds lacking hydrological data.

The studied basin was in southern Peru, where various lithological and hydro-geomorphological structures influence its flood vulnerability. To estimate flash flood vulnerability across all Caplina River micro-watersheds, 16 morphometric parameters were precisely analyzed, identifying areas of high vulnerability requiring watershed management measures.

To increase study reliability, a comparative analysis was conducted using PCA and WSA, finding that both techniques yielded similar results, although with some variations across micro-watersheds. In terms of model performance comparison, PCA is considered the more effective method for selecting the most effective parameters in micro-watershed prioritization evaluation, while WSA is time-consuming and less effective at identifying the most impactful factors regarding flash floods in micro-watersheds.

Results indicate that several micro-watersheds in the middle and lower sections of the basin exhibit high susceptibility to floods and soil erosion, leading to destructive impacts in the Caplina Basin. These findings underscore the necessity for targeted watershed management strategies, particularly in these high-risk areas, to mitigate flood impacts on agricultural land, infrastructure, and human settlements.

Finally, it can be stated that a basin's hydrological response, particularly the risk of flash floods and extreme events, is closely linked to its morphometric characteristics. Therefore, this methodology is proposed as a viable option for decision-makers implementing appropriate watershed management techniques, with a focus on soil and water conservation, enabling protection of the study area and mitigation of its degradation.

Acknowledgements

Thanks to the Jorge Basadre Grohmann National University, Tacna, Peru, Vice-Rectorate of Research and Research Institute for providing the canon, canon and mining royalties funds for the development of the project "Mitigation of the risk of overflow and flooding based on a proposal of assessment of sustainable public space in arid areas", approved with R.R. N°13626-2024-UNJBG. Also to H2O´UNJBG, Water Research Group.

Declaration of Interests

The authors declare that they have no conflict of interest.

Author Contributions

E. Pino-Vargas: Conceptualization, Formal analysis, Investigation, Writing-review, editing, Resources & Project administration. G. Huayna: Conceptualization, Investigation, Methodology, Writing-review & editing. Á. Tapia: Investigation, Writing-review & editing. V. Pocco: Investigation, Methodology. J. Espinoza-Molina: Formal analysis, Investigation, Project administration. F. Cabrera-Olivera: Visualization, Writing-review & editing. C. Huanacuni-Lupaca: Conceptualization, Writing-review & editing. K. Acosta-Caipa: Methodology, Writing-review. L. Ramos-Fernández: Methodology, Writing-review.

ORCID

E. Pino-Vargas https://orcid.org/0000-0001-7432-4364
G. Huayna https://orcid.org/0000-0002-4518-1023
A. Tapia https://orcid.org/0009-0009-9905-7077
V. Pocco https://orcid.org/0000-0001-9654-4499
J. Espinoza-Molina https://orcid.org/0000-0003-2236-8335
F. Cabrera-Olivera https://orcid.org/0000-0003-1429-8728
C. Huanacuni-Lupaca https://orcid.org/0000-0002-1148-4050
K. Acosta-Caipa https://orcid.org/0000-0003-1872-9062
L. Ramos-Fernández https://orcid.org/0000-0003-3946-7188

References

Abdelkareem, M., & Mansour, A. M. (2023). Risk assessment and management of vulnerable areas to flash flood hazards in arid regions using remote sensing and GIS-based knowledge-driven techniques. *Nat. Hazards*, *117*, 2269–2295. https://doi.org/10.1007/s11069-023-05942-x

Adeyeri, O. E., Folorunsho, A. H., Ayegbusi, K. I., Bobde, V., Adeliyi, T. E., Ndehedehe, C. E., & Akinsanola, A. A. (2024). Land surface dynamics and meteorological forcings modulate land surface temperature characteristics. *Sustain Cities Soc*, *101*, 105072. https://doi.org/10.1016/j.scs.2023.105072

Aggarwal, E., Whittaker, A. C., & Gupta, S. (2024). Investigating the influence of river geomorphology on human presence using night light data: A case study in the Indus Basin. *Remote Sens (Basel)*, *16*, 1272. https://doi.org/10.3390/rs16071272

Altaf, S., Meraj, G., & Romshoo, S. A. (2014). Morphometry and land cover based multi-criteria analysis for assessing the soil erosion susceptibility of the Western Himalayan Watershed. *Environ Monit Assess*, *186*, 8391–8412. https://doi.org/10.1007/s10661-014-4012-2

Amani, M., Ghorbanian, A., Ahmadi, S. A., Kakooei, M., Moghimi, A., Mirmazloumi, S. M., Moghaddam, S. H. A., Mahdavi, S., Ghahremanloo, M., Parsian, S., Wu, Q., Brisco, B. (2020) Google earth engine cloud computing platform for remote sensing big data applications: A comprehensive review. *IEEE J Sel Top Appl Earth Obs Remote Sens*, *13*, 5326–5350. https://doi.org/10.1109/jstars.2020.3021052

Balica, S. F., Douben, N., Wright, N. G. (2009). Flood vulnerability indices at varying spatial scales. *Water Sci. Technol.*, *60*, 2571–2580. https://doi.org/10.2166/wst.2009.183

Brêda, J. P. L. F., Cauduro Dias de Paiva, R., Siqueira, V. A., & Collischonn, W. (2023). Assessing climate change impact on flood discharge in South America and the influence of its main drivers. *J Hydrol (Amst)*, *619*, 129284. https://doi.org/10.1016/j.jhydrol.2023.129284

Bull, A. T., Andrews, B. A., Dorador, C., & Goodfellow, M. (2018). Introducing the Atacama Desert. *Antonie Van Leeuwenhoek*, *111*, 1269–1272. https://doi.org/10.1007/s10482-018-1100-2

Bush, S. A., Stallard, R. F., Ebel, B. A., & Barnard, H. R. (2020). Assessing plot-scale impacts of land use on overland flow generation in Central Panama. *Hydrol. Process*, *34*, 5043–5069. https://doi.org/10.1002/hyp.13924

Farr, T. G., Rosen, P. A., Caro, E., Crippen, R., Duren, R., Hensley, S., et al. (2007). The shuttle radar topography mission. *Reviews of Geophysics*, *45*. https://doi.org/10.1029/2005rg000183

Fernández-Nóvoa, D., González-Cao, J., & García-Feal, O. (2024). Enhancing flood risk management: A comprehensive review on flood early warning systems with emphasis on numerical modeling. *Water (Basel)*, *16*, 1408. https://doi.org/10.3390/w16101408

Gravelius, H., Flusskunde, G., & Verlagshan, D. B. (1914). Morphometry of drainage basins. Elsevier, Amsterdam 1914.

Horton, R. E. (1932). Drainage-basin characteristics. transactions, *American Geophysical Union*, *13*, 350–361. https://doi.org/10.1029/tr013i001p00350

Horton, R. E. (1914). Erosional development of streams and their drainage basins, hydrophysical approach to quantitative morphology. *Geol Soc Am Bull*, *56*, 275–370. https://doi.org/10.1130/0016-7606(1945)56[275:edosat]2.0.co;2

Hynek, S. A., McDowell, W. H., Bhatt, M. P., Orlando, J. J., & Brantley, S. L. (2022). Lithological control of stream chemistry in the Luquillo Mountains, Puerto Rico. *Front. Earth Sci.*, *10*. https://doi.org/10.3389/feart.2022.779459

Jolliffe, I. T., & Cadima, J. (2016). Principal Component Analysis: A review and recent developments. *Philos. Trans. R. Soc. A Math. Phys. Eng. Sci.*, *374*, 20150202. https://doi.org/10.1098/rsta.2015.0202

Kadam, A. K., Jaweed, T. H., Kale, S. S., Umrikar, B. N., & Sankhua, R. N. (2019). Identification of erosion-prone areas using modified morphometric prioritization method and sediment production rate: A remote sensing and GIS approach. *Geomatics, Natural Hazards and Risk*, *10*, 986–1006. https://doi.org/10.1080/19475705.2018.1555189

Kalogeropoulos, K., Tsanakas, K., Stathopoulos, N., Tsesmelis, D. E., &Tsatsaris, A. (2023). Cultural heritage in the light of flood hazard: The case of the "Ancient" Olympia, Greece. *Hydrology*, *10*, 61. https://doi.org/10.3390/hydrology10030061

Kumar, A., Singh, S., Pramanik, M., Chaudhary, S., Maurya, A. K., & Kumar, M. (2022). Watershed prioritization for soil erosion mapping in the lesser Himalayan Indian Basin using PCA and WSA methods in conjunction with morphometric parameters and GIS-Based approach. *Environ Dev Sustain*, *24*, 3723–3761. https://doi.org/10.1007/s10668-021-01586-8

Kundzewicz, Z. W., Su, B., Wang, Y., Wang, G., Wang, G., Huang, J., Jiang, T. (2019). Flood risk in a range of spatial perspectives – from global to local scales. *Natural Hazards And Earth System Sciences*, *19*, 1319–1328. https://doi.org/10.5194/nhess-19-1319-2019

Liu, H., Du, J., & Yi, Y. (2022). Reconceptualising flood risk assessment by incorporating sediment supply. *Catena (Amst)*, *217*, 106503. https://doi.org/10.1016/j.catena.2022.106503

Sreelakshmy, M., Dhanusree, M., & Thangamani, V. (2023). Application of GIS techniques to understand the geomorphometric characteristics of a tropical watershed in South India. *Geology, Ecology, and Landscapes*, *7*, 161–173. https://doi.org/10.1080/24749508.2021.1952749

Machaca-Pillaca, R., Pino-Vargas, E., Ramos-Fernández, L., Quille-Mamani, J., & Torres-Rua, A. (2022). Estimación de La evapotranspiración con fines de riego en tiempo real de un olivar a partir de imágenes de un drone en zonas áridas, caso La Yarada, Tacna, Perú. *Idesia (Arica)*, *40*, 55–65. https://doi.org/10.4067/s0718-34292022000200055

Mahala, A. (2020). The significance of morphometric analysis to understand the hydrological and morphological characteristics in two different morpho-climatic settings. *Appl Water Sci*, *10*, 33. https://doi.org/10.1007/s13201-019-1118-2

Meshram, S. G., & Sharma, S. K. (2017). Prioritization of watershed through morphometric parameters: A PCA-based approach. *Appl. Water Sci.*, *7*, 1505–1519. https://doi.org/10.1007/s13201-015-0332-9

Miller, V. C. (1953). Quantitative geomorphic study of drainage basin characteristics in the clinch mountain area, Virginia and Tennessee. Technical report (Columbia University. Department of Geology), no. 3 1953. https://doi.org/10.1086/626413

Ovalle, I. M., & Begazo, J. G. (2016). Organización del espacio y uso de los recursos naturales en la conformación de aldeas y campamentos en el período medio en los valles de Azapa, Norte de Chile y Caplina, Sur Del Perú. *Chungara, Revista de Antropología Chilena*, *48*, 531–555. https://doi.org/10.4067/s0717-73562016005000035

Piacentini, T., Carabella, C., Boccabella, F., Ferrante, S., Gregori, C., Mancinelli, V., Pacione, A., Pagliani, T., & Miccadei, E. (2020). Geomorphology-based analysis of flood critical areas in small hilly catchments for civil protection purposes and early warning systems: The case of the Feltrino Stream and the Lanciano Urban Area (Abruzzo, Central Italy). *Water (Basel)*, *12*, 2228. https://doi.org/10.3390/w12082228

Pike, R. J., & Wilson, S. E. (1971). Elevation-relief ratio, hypsometric integral, and geomorphic area-altitude analysis. *Geol Soc Am Bull*, *82*, 1079–1084. https://doi.org/10.1130/0016-7606(1971)82[1079:erhiag]2.0.co;2

Pinos, J., & Quesada-Román, A. (2021). Flood risk-related research trends in Latin America and the Caribbean. *Water (Basel)*, *14*, 10. https://doi.org/10.3390/w14010010

Pino-Vargas, E., & Chávarri-Velarde, E. (2022). Evidencias de cambio climático en la región hiperárida de la costa sur de Perú, cabecera del desierto de Atacama. *Tecnología y Ciencias Del Agua. 13*, 333–376. https://doi.org/10.24850/j-tyca-2022-01-08

Porto de Albuquerque, J., Anderson, L., Calvillo, N., Cattino, M., Clarke, A., Cunha, M. A., et al. (2023). Dialogic data innovations for sustainability transformations and flood resilience: The case for waterproofing data. *Global Environmental Change*, *82*, 102730. https://doi.org/10.1016/j.gloenvcha.2023.102730

Rentschler, J., Salhab, M., & Jafino, B. A. (2022). Flood exposure and poverty in 188 countries. *Nat Commun*, *13*, 3527. https://doi.org/10.1038/s41467-022-30727-4

Riaz, R., & Mohiuddin, M. (2025). Application of GIS-based multi-criteria decision analysis of hydro-geomorphological factors for flash flood susceptibility mapping in Bangladesh. *Water Cycle 2025*, *6*, 13–27. https://doi.org/10.1016/j.watcyc.2024.09.003

Roldán, F., Salazar, I., González, G., Roldán, W., & Toro, N. (2022). Flow-type landslides analysis in arid zones: Application in La Chimba Basin in Antofagasta, Atacama Desert (Chile). *Water (Basel)*, *14*, 2225. https://doi.org/10.3390/w14142225

Safanelli, J., Poppiel, R., Ruiz, L., Bonfatti, B., Mello, F., Rizzo, R., & Demattê, J. (2020). Terrain analysis in Google Earth Engine: A method adapted for high-performance global-scale analysis. *ISPRS Int J Geoinf*, *9*, 400. https://doi.org/10.3390/ijgi9060400

Schumm, S. A. (1956). Evolution of drainage systems and slopes in Badlands at Perth Amboy, New Jersey. *Geol Soc Am Bull*, *67*, 597–646. https://doi.org/10.1130/0016-7606(1956)67[597:eodsas]2.0.co;2

Sharma, N., Kaushal, A., Yousuf, A., Kaur, S., Sharda, R., Pal Singh, S., Gupta, O., & Sood, A. (2023). Prioritization of erosion susceptible watersheds using morphometric analysis and PCA approach: A case study of lower Sutlej River basin of Indian Punjab. *Watershed Ecology and the Environment*, *5*, 209–224. https://doi.org/10.1016/j.wsee.2023.08.002

Smith, K. G. (1950). Standards for grading texture of erosional topography. *Am J Sci*, *248*, 655–668. https://doi.org/10.2475/ajs.248.9.655

Sreedevi, P. D., Sreekanth, P. D., Khan, H. H., & Ahmed, S. (2013). Drainage morphometry and its influence on hydrology in an semi arid region: Using SRTM data and GIS. *Environ Earth Sci*, *70*, 839–848. https://doi.org/10.1007/s12665-012-2172-3

Strahler, A. N. (1964). Quantitative geomorphology of drainage basin and channel networks. Handbook of applied hydrology.

Thompson, A., & Clayton, J. (2002). The role of geomorphology in flood risk assessment. *Proceedings of the Institution of Civil Engineers - Civil Engineering*, *150*, 25–29. https://doi.org/10.1680/cien.2002.150.5.25

Vázquez-Tarrío, D., Ruiz-Villanueva, V., Garrote, J., Benito, G., Calle, M., Lucía, A., Díez-Herrero, A. (2024). Effects of sediment transport on flood hazards: Lessons learned and remaining challenges. *Geomorphology*, *446*, 108976. https://doi.org/10.1016/j.geomorph.2023.108976

Velliangiri, S., Alagumuthukrishnan, S., & Thankumar joseph, S. I. (2019). A review of dimensionality reduction techniques for efficient computation. *Procedia Comput Sci*, *165*, 104–111. https://doi.org/10.1016/j.procs.2020.01.079

Wei, L., Hu, K., & Liu, J. (2021). Quantitative analysis of the debris flow societal risk to people inside buildings at different times: A case study of Luomo Village, Sichuan, Southwest China. *Front Earth Sci (Lausanne)*, *8*. https://doi.org/10.3389/feart.2020.627070

Willgoose, G. (1994). A Physical explanation for an observed area-slope-elevation relationship for catchments with declining relief. *Water Resour Res*, *30*, 151–159. https://doi.org/10.1029/93wr01810

Wold, S., Esbensen, K., & Geladi, P. (1987). Principal Component Analysis. *Chemometrics and Intelligent Laboratory Systems*, *2*, 37–52. https://doi.org/10.1016/0169-7439(87)80084-9

Yadav, S. K., Dubey, A., Singh, S. K., & Yadav, D. (2020). Spatial regionalisation of morphometric characteristics of mini watershed of Northern Foreland of Peninsular India. *Arabian Journal of Geosciences*, *13*, 435. https://doi.org/10.1007/s12517-020-05365-z

Zheng, Y., Yu, C., Zhou, H., & Xiao, J. (2021). Spatial variations and influencing factors of river networks in river basins of China. *Int. J. Environ. Res. Public Health*, *18*, 11910. https://doi.org/10.3390/ijerph182211910